

Influence of Defect States and Thickness of Interface Layer On High Efficiency of c-Si/a-Si:H Heterojunction Solar Cells With Higher Bandgap a-Si:H(p) Layer By Simulation

Venkanna Kanneboina (✉ venkanna@alumni.iitg.ac.in)

St. Martin's Engineering College <https://orcid.org/0000-0002-8351-9670>

Research Article

Keywords: c-Si/a-Si:H heterojunction solar cells, Interface, Thickness, Defect density, Simulation

Posted Date: February 22nd, 2021

DOI: <https://doi.org/10.21203/rs.3.rs-210502/v1>

License:  This work is licensed under a Creative Commons Attribution 4.0 International License.

[Read Full License](#)

Abstract

This paper presents the influence of defect states and thickness of interface layer on high efficiency of c-Si/a-Si:H heterojunction solar cells with higher bandgap emitter a-Si:H(p) layer by AFORS-HET simulation tool. At first, the performance of *Ag/ZnO/a-Si:H(p)/a-Si:H(i)/c-Si(n)/a-Si:H(i)/a-Si:H(n)/Ag* heterojunction solar cells was studied by altering the thickness of a-Si:H(p) and a-Si:H(i) layers. The best values of open circuit voltage (V_{oc}) (764.8 mV), short circuit current density (J_{sc}) (43.15 mA/cm²), fill factor (FF) (85.71) and efficiency (η) (28.28%) were obtained at 3 nm of a-Si:H(p) and a-Si:H(i) layer. In the same structure, c-Si(n) interface was introduced in between c-Si(n) and a-Si:H(i) layer. It is found that the solar cell performance was not changed by varying defect density from 10^9 - 10^{14} cm⁻³ for thin (5 and 10 nm) interface layer and estimated values are 761.7 mV, 38.83 mA/cm², 86.09%, 25.46% correspond to V_{oc} , J_{sc} , FF, η respectively. For very thick interface layer, defect density has shown huge impact on the device performance. At 1 μm, the V_{oc} , FF and η values have been changed from 760.2 to 653.2 mV, 85.9 to 80.76% and 22.94 to 18.47% for the defect density of 10^9 to 10^{14} cm⁻³ respectively.

1. Introduction

Solar energy will be the main energy source in future due to drastic changes in geographical and environmental conditions. The solar renewable energy is best alternate among all other renewable energy sources. The crystalline silicon (c-Si) photovoltaic (PV) technology is dominating the market with a share of 95% in the present days and it is likely to continue in forthcoming years also due to its durability, stability, abundance, environment friendly and higher efficiency, whereas, other thin film technology is about 5% of market share [1] and in this 5%, a-Si:H thin film based solar cells accounted 0.3% [1] due to higher defect density, instability of material [2] and low conversion efficiency of solar cells [3]. The crystalline silicon and amorphous Si heterojunction solar cells have been suggested for best alternate to crystalline silicon solar cells. These c-Si/a-Si:H heterojunction solar cells can be easily fabricated at temperature below 200°C, whereas, junction formation in conventional c-Si solar cells is usually done by a thermal diffusion step, for which temperature of 800-1000 °C is needed [4]. In 2014, The Sanyo has published best efficiency of 25.6% [5] and V_{oc} of 750 mV on n-doped c-Si with double side HIT structure [6]. Currently many research groups are working on c-Si/a-Si:H heterojunctions solar cells to improve the performance by addressing many issues which are responsible for deterioration of the performance of the cells [3, 7].

The performance of the c-Si/a-Si:H heterojunction solar cells depends on many parameters such as substrate cleaning, recombination and optical losses, interface defects, series and shunt resistances, quality of a-Si:H and TCO layers and metal contacts. It is very important to study the interface layers to eliminate recombination issues and ameliorate transportation of charge carriers for silicon heterojunction solar cells.

Numerical simulation is very useful method to evaluate and understand the device performance by designing the various solar cell structures and varying parameters such as thickness, interface defects, bandgap, defect density of a-Si:H layers and c-Si substrates, different transparent conducting oxide layers, work function of the layers [8–16]. This simulation can give understanding of the concepts, save lots money and time before starting the experimental trials to fabricate devices and improve the device performance. There are several simulation tools available to evaluate and understand the solar cell performance such as AFORS-HET [12, 16, 17], AMPS [18], Sentaurus [19], Scaps [20], Silvano [21], Asa [22], Lumerical FDTD [23, 24] etc. Among these tools, AFORHET is most useful simulation tool for c-Si/a-Si:H heterojunction solar cells [12, 25, 26]. Many researcher groups have modeled several devices and analyzed by varying thickness of layers, bandgap, interface defect states, doping concentration [27–29]. Louis O. Antwi et.al achieved simulation efficiency of 29.19% with optimization of the defects and defined charge density of interfaces [30]. Dwivedi et.al obtained simulation efficiency of 27% by modeling different thickness of layers of various structures [31]. However, most of the researchers used the bandgap of p-layer 1.7 eV in the simulation [13, 32–35]. This band gap is almost 0.1-0.2 eV lower for boron doped a-Si:H films, which are deposited by experimental methods.

In this paper, c-Si/a-Si:H heterojunction structure of Ag/ZnO/a-Si:H(p)/ a-Si:H(i)/ c-Si(n)/ a-Si:H(i)/ a-Si:H(n)/Ag was simulated with a high band gap a-Si:H(p) layer by *AFORSHEt* auto machine tool. First, analyzed the how the thickness of a-Si:H(p) and a-Si:H(i) affect the solar cell parameters such as V_{oc} , J_{sc} , FF and η . Next, c-Si(n) interface layer was introduced in between c-Si(n) substrate and a-Si:H(i) layer to analyze how defect states and thickness of interface layer affect the performance of solar cell devices. Generally, the thickness of c-Si wafer was in the range of 200-300 μm and it is not constant throughout the wafer. The defect density on surface and bulk will vary from one position to other position. It is very important to understand the interface near c-Si wafer, whereas, a-Si:H(i) layer thickness is in the range of 4-10 nm only.

2. Simulation Details

AFORSHEt is used for modeling of c-Si/a-Si:H heterojunction solar cells. The solar radiation of AM 1.5G with incident power of 100 mW/cm² and flat band metal contacts were used in this simulation work. The input parameters for c-Si/a-Si:H hetero structure solar cells are given in the Table 1[12, 16, 17, 26, 27, 31, 36–39]. The density of states distribution for c-Si(n), a-Si:H(p), a-Si:H(i) and a-Si:H(n) are shown in Figure 2 (a-d respectively) [10, 12, 16, 31, 40]. The other parameters are used as preset default values in *AFORSHEt* software [31, 36]. The schematic diagram of c-Si/a-Si:H heterojunction solar cell structure was shown in Figure 1. Thickness of a-Si:H(i) and a-Si:H(p) layers were varied and evaluated the solar cell performance for structure shown in Figure 1a. The high bandgap (1.8 eV) of p-layer was used for both structures in this work. The i- and p-layer thickness was optimized and this optimized thickness was used in second structure (Figure 1b). The c-Si(n) interface layer was introduced in between c-Si and i-layer (Figure 1b). The thickness and defect density of this interface layer has been varied and remaining parameters used as same as c-Si(n). Thickness and defect density were varied in the range of 5, 10, 50,

100, 150, 250, 450, 750 and 1000 nm and 10^9 to 10^{14} cm $^{-3}$ respectively for second c-Si/a-Si:H heterojunction solar cell structure (Figure 1b).

Table 1. Input parameters used in the present simulation for c-Si/a-Si:H heterojunction solar cells.

parameter	c-Si(n)	a-Si:H(p)	a-Si:H(i)	a-Si:H(n)
Thickness	250 μm	Variable	variable	5 nm
Dielectric constant	11.1	11.1	11.1	11.1
Electron affinity (eV)	4.05	3.9	3.9	3.9
Bandgap (eV)	1.12	1.8	1.72	1.72
Effective conduction band density (cm $^{-3}$)	2.8×10^{19}	6.9×10^{20}	6.9×10^{20}	6.9×10^{20}
Effective valence band density (cm $^{-3}$)	2.8×10^{19}	1.2×10^{21}	1.2×10^{21}	1.2×10^{21}
Electron mobility (cm 2 V $^{-1}$ s $^{-1}$)	1321	7	7	7
Hole mobility (cm 2 V $^{-1}$ s $^{-1}$)	461	1	1	1
Acceptor concentration (cm $^{-3}$)	0	6.1×10^{21}	0	
Donor concentration (cm $^{-3}$)	5×10^{16}	0	0	1.7×10^{21}
Thermal velocity of electrons (cm s $^{-1}$)	10^7	10^7	10^6	10^7
Thermal velocity of holes (cm s $^{-1}$)	10^7	10^7	10^6	10^7
Layer density (g cm $^{-3}$)	2.328	2.328	2.328	2.328
Auger recombination coefficient for electron (cm 6 s $^{-1}$)	2.2×10^{-31}	0	0	0
Auger recombination coefficient for hole (cm 6 s $^{-1}$)	9.9×10^{-32}	0	0	0
Direct band-to-band recombination coefficient (cm 3 s $^{-1}$)	9.5×10^{-15}	0	0	0

3. Results And Discussion

3.1 Optimization of thickness of a-Si:H(i) layer

Figure 4 shows the variation of a-Si:H(i) layer thickness with solar cell parameters. The thickness of a-Si:H(i) layer was varied from 3 to 20 nm. The thickness of p-layer was fixed at 5 nm for this i-layer optimization. The V_{oc} of 763.3 mV, J_{sc} of 42.17, FF 85.77 and η of 27.6 obtained for 3 nm of i-layer. It was found that the V_{oc} values are not changed up to 10 nm and slightly increased at 15 and 20 nm of i-layer. The V_{oc} of solar cells mainly depends on bulk and interface defects and also recombination centers. It is observed that the J_{sc} values are decreased as increase in thickness of i-layer. The J_{sc} values are decreased to 40.41 from 42.17 mA/cm 2 . This is mainly due to increased absorption of photons in the i-layer while entering into c-Si substrate. As a results in less number of free electron-hole generation. After generation, free carriers travel through i-layer to reach metal contacts, in this process, these free carriers recombine in the i-layer due to large minority carrier path length of i-layer [37]. The FF values are not changed up to 10 nm of i-layer and beyond that FF values are decreased due to increased resistance of thick i-layer. The maximum efficiency of 27.6% was obtained at 3 nm of i-layer. These values are decreased as increase in thickness of i-layer due to decrease of J_{sc} and FF of solar cells. The efficiency of 23.62% was obtained at 20 nm thick i-layer.

3.2 Optimization of thickness of a-Si:H(p) layer

Figure 5 shows the variation of a-Si:H(p) layer thickness with solar cell parameters. The thickness of a-Si:H(p) layer was varied from 3 to 20 nm and thickness of i-layer was fixed at 3nm, where obtained best efficiency was 27.6%. The V_{oc} of 764.8 mV, J_{sc} of 43.15, FF of 85.71 and η of 28.28% were obtained for 3 nm of p-layer. In order to match the more realistic experimental bandgap value of p-layer, the bandgap of p-layer was kept at 1.8 eV. The maximum value of V_{oc} (764.8 mV) was obtained at 3 nm of p-layer and it was decreased as increase in the thickness of p-layer. The reason is that increased defect density in the p-layer with increase in the thickness of p-layer [27, 33]. The V_{oc} decreased from 764.8 mV to 760.2 mV as increase of p-layer thickness of 3- 20 nm respectively. The high J_{sc} of 43.15 mA/cm² obtained at 3 nm of p-layer thickness. Absorption losses were reduced with less thickness p-layer. The higher bandgap p-layer allows more number photons to reach c-Si substrate, which results in high J_{sc} values in the solar cells. The FF values are not changed much as increase in thickness. The increase in V_{oc} , J_{sc} and FF values of solar cells resulting in an increased efficiency of solar cells with decreasing thickness of p-layer. The low value of efficiency 24.21% obtained at 20 nm thick p-layer.

3.3. Influence of thickness of interface layer at different defect density

The c-Si(n) interface was introduced between i-layer and c-Si substrate in the c-Si/a-Si:H heterojunction solar cells. The defect density on surface and bulk of the c-Si wafer is not equally distributed and this defect density may vary with fabrication, wafer processing and thickness of wafer [5, 6, 41]. Usually, thickness of the wafer is more at centre and less at edges of diameter. In order to study the effect of defect density and thickness on c-Si/a-Si:H heterojunction solar cells, the defect density and thickness of c-Si(n) interface layer was varied from 10^9 - 10^{14} cm⁻³ and 5 nm-1 μ m respectively. The 250 μ m thick c-Si was used in this study. The 5-10 nm, 50 nm thin and 0.1 to 1 μ m thick interface layer was introduced at different defect density (10^9 - 10^{14} cm⁻³).

Figure 6 (a-f) show the performance of c-Si/a-Si:H heterojunction solar cell with c-Si(n) interface layer thickness at defect density (10^9 - 10^{14} cm⁻³) of interface. Figure 6a shows the solar cell parameters as a function of the thickness at the defect density 10^9 cm⁻³ of c-Si(n) interface. The V_{oc} is not changed up to 150 nm of interface layer and then it was decreased at 0.25 μ m, further, V_{oc} was constant till 1 μ m thick interface layer. The J_{sc} values are decreased from 38.83 to 35.14 mA/cm² as thickness increased. Absorption losses in solar cells were increased by increasing thickness of interface layer. The changes in FF are very less with thickness at the defect density of 10^9 cm⁻³ of interface. The resulting efficiency has decreased. The achieved V_{oc} , J_{sc} , FF, η is 761.7 mV, 38.83 mA/cm², 86.11%, 25.47% and 760.2, 35.14, 85.9%, 22.94% at 5 nm and 1 μ m thick interface layer respectively. In previous section, it is observed that even 20 nm thick a-Si:H layer has huge impact on the performance of the solar cell. In Figure 6b, at the defect density of 10^{10} cm⁻³, the performance of solar cells has not changed and almost equally comparable with the performance at the defect of 10^9 cm⁻³. At the defect density of 10^{11} cm⁻³ in Figure 6c, the V_{oc} (761.7 mV) has not changed till 150 nm thick layer and later decreased gradually. The V_{oc} has decreased to 758.6 mV at 1 μ m thick interface layer and J_{sc} and FF have followed similar trend of earlier

solar cells. Slight decrease in efficiency has been observed at 1 μm of interface layer due to decrease in V_{oc} . The achieved V_{oc} , J_{sc} , FF , η is 761.7 mV, 38.83 mA/cm 2 , 86.11%, 25.47% and 758.6, 35.14, 85.83%, 22.88% at 5 nm and 1 μm thick interface layer respectively at the defect of 10^{11} cm^{-3} of interface. In Figure 6d, the performance of the c-Si/a-Si:H solar cell have not changed till 150 nm thick at defect density of 10^{12} cm^{-3} . Then slightly decreased at 250 and 450 nm thickness. The V_{oc} and efficiency have decreased to 750 mV and 22.88% with 10^{12} cm^{-3} at 1 μm of interface layer respectively. The solar parameters were not changed at 5 and 10 nm even at high defect density of 10^{13} cm^{-3} (Figure 6e). The V_{oc} and FF have not changed at thin layer of 5 nm and 10 nm and then V_{oc} of 4 mV and 8 mV decreased at 50 nm and 100 nm respectively at the defect of 10^{13} cm^{-3} of interface (Figure 6e). The V_{oc} has been decreased significantly as increase in thickness beyond 100 nm and severely affected with 10^{13} cm^{-3} at 1 μm of interface layer. Very low V_{oc} of 713 mV observed at 1 μm and the J_{sc} has not changed at high defect density as variation of thickness of interface layer. The FF values are decreased up to 100 nm and then slightly increased further increase in the thickness of the interface layer.

The efficiency of cells decreased with thickness and low efficiency of 20.54% observed at 1 μm . The solar cell parameters were not significantly changed at 5 and 10 nm of c-Si interface layer even at high defect density of 10^{14} cm^{-3} (Figure 6f). The J_{sc} values are not changed with defect density. The FF values are decreased and then increased slightly. The V_{oc} was significantly decreased from the thickness of 150 nm to 1 μm . The lowest V_{oc} and η of 652.3 mV and 18.47% were observed with 1 μm respectively. The achieved V_{oc} , J_{sc} , FF , η is 761.7 mV, 38.83 mA/cm 2 , 86.09%, 25.46% and 652.3, 35.05, 80.76%, 18.47% at 5 nm and 1 μm thick interface layer respectively at the defect of 10^{14} cm^{-3} of interface.

3.4. Influence of defect density of interface layer at different thickness

Figure 7 (a-i) show the solar cell parameters as a function of c-Si(n) interface layer defect density at different thickness of interface layer respectively. Solar cell parameters were estimated by varying defect density from 10^9 to 10^{14} cm^{-3} at different thicknesses such as 5, 10, 50, 150, 200, 450, 750 and 1000 nm. It was observed that at 5 and 10 nm thick, solar cell parameters V_{oc} , J_{sc} , FF and efficiency were not changed for defect density (10^9 to 10^{14} cm^{-3}) of c-Si(n) interface layer (Figure 7(a, b)). This means that defect density is not affecting at very thin interface layer. The obtained values V_{oc} , J_{sc} , FF , η at 10^{14} cm^{-3} are 761.7 mV, 38.83 mA/cm 2 , 86.09%, 25.46% and 761.7 mV, 38.75 mA/cm 2 , 85.95%, 25.37% for 5, 10 nm respectively (Figure 7(a, b)). In Figure 7(c, d), the V_{oc} , J_{sc} , FF and η values are not changed up to 10^{12} cm^{-3} of defect density and the performance of the solar cell was deteriorated as further increase in the defect density. The defect density of 10^{12} cm^{-3} is maximum limit for 50, 100 and 150 nm thick interface layer for less changes in solar cell parameters. The obtained values of V_{oc} , J_{sc} , FF , η at 10^{12} cm^{-3} are 761.7 mV, 38.26 mA/cm 2 , 85.81%, 25% and 760.2 mV, 37.77 mA/cm 2 , 85.76% FF, 24.62%, 760.2 mV, 37.38 mA/cm 2 , 85.6%, 24.32% for 50, 100 and 150 nm respectively (Figure 7(c-e)). The performance of solar cells was not changed in the range of 10^9 to 10^{11} cm^{-3} of defect density and beyond these density

V_{oc} , FF and J_{sc} has decreased at thickness of 250 nm (Figure 6f). In Figure 7(g, h), the efficiency has decreased about 2% at 10^9 and 10^{10} cm^{-3} , this continued up to 10^{12} cm^{-3} of defect density. The obtained values of V_{oc} , J_{sc} , FF, efficiency at 10^{10} cm^{-3} are 760.2 mV, 36.02 mA/cm², 85.98%, 23.54% and 760.2 mV, 35.42 mA/cm², 85.91%, 23.13% for 450 and 750 nm respectively. The obtained low values of V_{oc} , J_{sc} , FF, J_{sc} at 10^{14} cm^{-3} are 671.1 mV, 36.01 mA/cm², 81.21%, 19.62% and 658.6.2 mV, 35.37 mA/cm², 81.24%, 18.93% for 450 and 750 nm respectively. The current density has not changed by varying defect density from 10^9 to 10^{14} cm^{-3} at each thickness of interface. In Figure 7i, at 1000nm, the V_{oc} , FF and efficiency values have been changed from 760.2 to 653.2 mV, 85.9 to 80.76% and 22.94 to 18.47% for 10^9 to 10^{14} cm^{-3} of defect density. It is found that the solar cell performance was not deteriorated with very thin (5 and 10 nm) c-Si(n) interface layer for defect density in the range of 10^9 to 10^{14} cm^{-3} . For the 50-150 nm thick interface layer, the solar cell parameters values decreased slightly due to thickness of interface layer and however performance was not effected by defect density in the range 10^9 to 10^{12} cm^{-3} and beyond this defect density, solar cell parameter values are decreased. The performance of solar cells was not affected till the defect density of 10^{12} cm^{-3} for the thickness of interface layer of 250 and 450 nm . The solar cell performance was severely deteriorated by very thick interface layer even at low defect density.

The current density of solar cells was decreased as thickness increased and it was not changed with defect density of interface layer. For very thin interface layer, the V_{oc} and FF, efficiency values are not changed by varying defect density. However, the V_{oc} values are severely affected by high defect density for very thin interface layer. In very thin layer, generated charge carriers crossed junction without recombining at interface. Whereas in the case of thick and very thick interface layer, recombination centres increased and generated and separated charge carriers recombined at interface layer before crossing the junction and reaching metal contacts. The FF values are decreased as increase in thickness of interface layer due to increased resistance losses in the solar cells. Resulting efficiency of solar cells was decreased as increase in thickness and defect density of interface layer.

4. Conclusion

The $\text{Ag}/\text{ZnO}/\text{a-Si:H}(p)/\text{a-Si:H}(i)/\text{c-Si}(n)/\text{a-Si:H}(i)/\text{a-Si:H}(n)/\text{Ag}$ solar cell has been successfully designed and evaluated by AFORS-HET simulation tool. The higher bandgap (1.8 eV) of a-Si:H(p) was used in this work. The performance of c-Si/a-Si:H heterostructure was studied by varying the thickness of a-Si:H(p) and a-Si:H(i) layers. The best values of V_{oc} (764.8 mV), J_{sc} (43.15 mA/cm²), FF (85.71%) and efficiency (28.28%) were obtained at 3 nm of a-Si:H(p) and a-Si:H(i) layer. In the same structure, c-Si(n) interface layer was introduced in between c-Si(n) substrate and a-Si:H(i) layer. Studied the performance of c-Si/a-Si:H heterojunction solar cells by varying defect density and thickness from 10^9 to 10^4 cm^{-3} and very thin (5 nm) to thick (1 μm) of interface layer respectively. The less defective interface improves the solar cell performance. The achieved V_{oc} , J_{sc} , FF, J_{sc} is 761.7 mV, 38.83 mA/cm², 86.11%, 25.47% and 760.2, 35.14, 85.9%, 22.94% at 5 nm and 1 μm thick interface layer respectively at the defect density of 10^9 cm^{-3} of interface. The efficiency of about 2% has decreased as increase in thickness from 5 nm to 1 μm. It is

found that the solar cell performance was not changed by varying defect density from 10^9 - 10^{14} cm $^{-3}$ for thin interface layer. The estimated values are 761.7 mV, 38.83 mA/cm 2 , 86.09% and 25.46% correspond to V_{oc} , J_{sc} , FF and η for 5 and 10 nm thick interface having the defect density range of 10^9 - 10^{14} cm $^{-3}$ respectively. At 1000 nm, the V_{oc} , FF and efficiency values have been changed from 760.2 to 653.2 mV, 85.9 to 80.76% and 22.94 to 18.47% for the defect density of 10^9 to 10^{14} cm $^{-3}$ respectively. For the very thin interface layer, defect density has not shown significant effect on device performance. This could be due to generated free charges carriers immediately reaching metal contacts without recombining in the very thin interface layer. Defect density has huge impact on the device performance for very thick interface layer. The V_{oc} and efficiency decreased significantly even at low defect density of 10^9 cm $^{-3}$. This could be due to large recombination losses in the very thick layer of interface.

Declarations

Acknowledgment

Authors also acknowledge Helmholtz-Zentrum Berlin for providing AFORS-HET simulation software.

Funding statement: No funding was received for conducting this study

Author contributions: Conceptualization, Data curation, Formal analysis, Investigation, Methodology, Software, Writing - original draft, Writing - review & editing.

Availability of data and material: The data that support the findings of this study are available from the corresponding author upon reasonable request.

Compliance with ethical standards: The authors declare that they have no known competing financial interests or personal relationships that could have appeared to influence the work reported in this paper.

Consent to participate: Not applicable

Consent to publication: The Author hereby confirms the consent to publication of the work in Silicon journal.

References

1. Fraunhofer Institute for Solar Energy Systems (2018) Photovoltaics Report, 27 August 2018
2. R.A.Street (1991) Hydrogenated amorphous silicon
3. Green MA, Hishikawa Y, Dunlop ED, et al (2018) Solar cell efficiency tables (version 52). *Prog Photovoltaics Res Appl* 26:427–436. <https://doi.org/10.1002/pip.3040>
4. Zhao J, Wang A, Green MA (2001) High-efficiency PERL and PERT silicon solar cells on FZ and MCZ substrates. *Sol Energy Mater Sol Cells* 65:429–435. [https://doi.org/10.1016/S0927-0248\(00\)00123-9](https://doi.org/10.1016/S0927-0248(00)00123-9)

5. Masuko K, Shigematsu M, Hashiguchi T, et al (2014) Achievement of More Than 25% Conversion Efficiency With Crystalline Silicon Heterojunction Solar Cell. *IEEE J Photovoltaics* 4:1433–1435. <https://doi.org/10.1109/JPHOTOV.2014.2352151>
6. Taguchi M, Yano A, Tohoda S, et al (2014) 24.7% Record efficiency HIT solar cell on thin silicon wafer. *IEEE J Photovoltaics* 4:96–99. <https://doi.org/10.1109/JPHOTOV.2013.2282737>
7. NREL (2018) NREL Efficiency Chart. <https://www.nrel.gov/pv/assets/pdfs/pv-efficiencies-07-17-2018.pdf> (accessed Sep 20, 2018)
8. Gudovskikh AS, Ibrahim S, Kleider JP, et al (2007) Determination of band offsets in a-Si:H/c-Si heterojunctions from capacitance-voltage measurements: Capabilities and limits. *Thin Solid Films* 515:7481–7485. <https://doi.org/10.1016/j.tsf.2006.11.198>
9. Korte L, Conrad E, Angermann H, et al (2008) The a-Si:H/c-Si interface - key for high efficiency heterojunction cells. *J Non Cryst Solids* 354:2138
10. Zhao L, Zhou CL, Li HL, et al (2008) Design optimization of bifacial HIT solar cells on p-type silicon substrates by simulation. *Sol Energy Mater Sol Cells* 92:673–681. <https://doi.org/10.1016/j.solmat.2008.01.018>
11. Mikolášek M, Racko J, Harmatha L, et al (2010) Influence of the broken symmetry of defect state distribution at the a-Si:H/c-Si interface on the performance of hetero-junction solar cells. *Appl Surf Sci* 256:5662–5666. <https://doi.org/10.1016/j.apsusc.2010.03.023>
12. Stangl R, Leendertz C, Haschke J (2010) Numerical Simulation of Solar Cells and Solar Cell Characterization Methods: the Open-Source on Demand Program AFORS-HET
13. Cruz A, Wang EC, Morales-Vilches AB, et al (2019) Effect of front TCO on the performance of rear-junction silicon heterojunction solar cells: Insights from simulations and experiments. *Sol Energy Mater Sol Cells* 195:339–345. <https://doi.org/10.1016/j.solmat.2019.01.047>
14. Belfar A (2015) The role of p+-layer dopant concentration, p+-layer band gap and p+-layer thickness in the performances of a-Si:H n - I - p - P+ solar cells with double layer window nanocrystalline silicon. *Optik (Stuttg)* 126:5688–5693. <https://doi.org/10.1016/j.ijleo.2015.09.026>
15. Belfar A (2015) Simulation study of the a-Si:H/nc-Si:H solar cells performance sensitivity to the TCO work function, the band gap and the thickness of i-a-Si:H absorber layer. *Sol Energy* 114:408–417. <https://doi.org/10.1016/j.solener.2015.02.010>
16. Venkanna Kanneboina (2020) The simulated performance of c-Si/a-Si:H heterojunction solar cells with nc-Si:H, μc-Si:H, a-SiC:H, and a-SiGe:H emitter layers. *J Comput Electron.* <https://doi.org/10.1007/s10825-020-01626-y>
17. Varache R, Kleider JP, Gueunier-Farret ME, Korte L (2013) Silicon heterojunction solar cells: Optimization of emitter and contact properties from analytical calculation and numerical simulation. *Mater Sci Eng B Solid-State Mater Adv Technol* 178:593–598. <https://doi.org/10.1016/j.mseb.2012.11.011>
18. Hernández-Como N, Morales-Acevedo A (2010) Simulation of hetero-junction silicon solar cells with AMPS-1D. *Sol Energy Mater Sol Cells* 94:62–67. <https://doi.org/10.1016/j.solmat.2009.05.021>

19. Wu YC, Jhan YR (2017) 3D TCAD simulation for CMOS nanoelectronic devices
20. Mostefaoui M, Mazari H, Khelifi S, et al (2015) Simulation of High Efficiency CIGS Solar Cells with SCAPS-1D Software. *Energy Procedia* 74:736–744. <https://doi.org/10.1016/j.egypro.2015.07.809>
21. Vergura S (2015) Scalable model of PV cell in variable environment condition based on the manufacturer datasheet for circuit simulation. 2015 IEEE 15th Int Conf Environ Electr Eng EEEIC 2015 - Conf Proc 1481–1485. <https://doi.org/10.1109/EEEIC.2015.7165390>
22. Pieters BE, Krc J, Zeman M (2006) Advanced numerical simulation tool for solar cells - ASA5. Conf Rec 2006 IEEE 4th World Conf Photovolt Energy Conversion, WCPEC-4 2:1513–1516. <https://doi.org/10.1109/WCPEC.2006.279758>
23. Shin SC, Koh CW, Vincent P, et al (2019) Ultra-thick semi-crystalline photoactive donor polymer for efficient indoor organic photovoltaics. *Nano Energy* 58:466–475. <https://doi.org/10.1016/j.nanoen.2019.01.061>
24. Vincent P, Kim DK, Kwon JH, et al (2018) Correlating the nanoparticle size dependent refractive index of ZnO optical spacer layer and the efficiency of hybrid solar cell through optical modelling. *Thin Solid Films* 660:558–563. <https://doi.org/10.1016/j.tsf.2018.06.004>
25. Wang L, et al. (2011) Simulation of High Efficiency Heterojunction Solar Cells with AFORS-HET. *J Phys Conf Ser* 276:12177. <https://doi.org/10.1088/1742-6596/276/1/012177>
26. Stangl R, Kriegel M, Schmidt M (2007) AFORS-HET, version 2.2, a numerical computer program for simulation of heterojunction solar cells and measurements. Conf Rec 2006 IEEE 4th World Conf Photovolt Energy Conversion, WCPEC-4 2:1350–1353. <https://doi.org/10.1109/WCPEC.2006.279681>
27. Schropp REI, Zeman M (1998) Amorphous and Microcrystalline Silicon Solar Cells: Modeling, Materials and Device Technology
28. Ali A, Gouveas T, Hasan M -a., et al (2011) Influence of deep level defects on the performance of crystalline silicon solar cells: Experimental and simulation study. *Sol Energy Mater Sol Cells* 95:2805–2810. <https://doi.org/10.1016/j.solmat.2011.05.032>
29. Aksari MB, Eray A (2011) Optimization of a-Si:H/c-Si heterojunction solar cells by numerical simulation. *Energy Procedia* 10:101–105. <https://doi.org/10.1016/j.egypro.2011.10.160>
30. Oppong-Antwi L, Huang S, Li Q, et al (2017) Influence of defect states and fixed charges located at the a-Si:H/c-Si interface on the performance of HIT solar cells. *Sol Energy* 141:222–227. <https://doi.org/10.1016/j.solener.2016.11.049>
31. Dwivedi N, Kumar S, Bisht A, et al (2013) Simulation approach for optimization of device structure and thickness of HIT solar cells to achieve ~27% efficiency. *Sol Energy* 88:31–41. <https://doi.org/10.1016/j.solener.2012.11.008>
32. Qiu D, Duan W, Lambertz A, et al (2020) Front contact optimization for rear-junction SHJ solar cells with ultra-thin n-type nanocrystalline silicon oxide. *Sol Energy Mater Sol Cells* 209:110471. <https://doi.org/10.1016/j.solmat.2020.110471>
33. Sharma M, Kumar S, Dwivedi N, et al (2013) Optimization of band gap, thickness and carrier concentrations for the development of efficient microcrystalline silicon solar cells: A theoretical

- approach. Sol Energy 97:176–185. <https://doi.org/10.1016/j.solener.2013.08.012>
34. Wen X, Zeng X, Liao W, et al (2013) An approach for improving the carriers transport properties of a-Si:H/c-Si heterojunction solar cells with efficiency of more than 27%. Sol Energy 96:168–176. <https://doi.org/10.1016/j.solener.2013.07.019>
35. Morales-Acevedo A, Hernández-Como N, Casados-Cruz G (2012) Modeling solar cells: A method for improving their efficiency. Mater Sci Eng B 177:1430–1435. <https://doi.org/10.1016/j.mseb.2012.01.010>
36. Varache R, Leendertz C, Gueunier-Farret ME, et al (2015) Investigation of selective junctions using a newly developed tunnel current model for solar cell applications. Sol Energy Mater Sol Cells 141:14–23. <https://doi.org/10.1016/j.solmat.2015.05.014>
37. Singh S, Kumar S, Dwivedi N (2012) Band gap optimization of p-i-n layers of a-Si:H by computer aided simulation for development of efficient solar cell. Sol Energy 86:1470–1476. <https://doi.org/10.1016/j.solener.2012.02.007>
38. Stangl R, Kriegel M, Schmidt M (2006) Afors-Het, a Numerical Pc-Program for Simulation of (Thin Film) Heterojunction Solar Cells, Version 2.0 (Open-Source on Demand), To Be Distributed for Public Use. Proceedings 1:1–4
39. Stangl RA AFORS HET 3 . 0 first approach to a two dimensional simulation of solar cells. 0–5
40. Yao Y, Xu X, Zhang X, et al (2018) Enhanced efficiency in bifacial HIT solar cells by gradient doping with AFORS-HET simulation. Mater Sci Semicond Process 77:16–23. <https://doi.org/10.1016/j.mssp.2018.01.009>
41. De Wolf S, Descoedres A, Holman ZC, Ballif C (2012) High-efficiency Silicon Heterojunction Solar Cells: A Review. Green 2:7–24. <https://doi.org/10.1515/green-2011-0018>

Figures

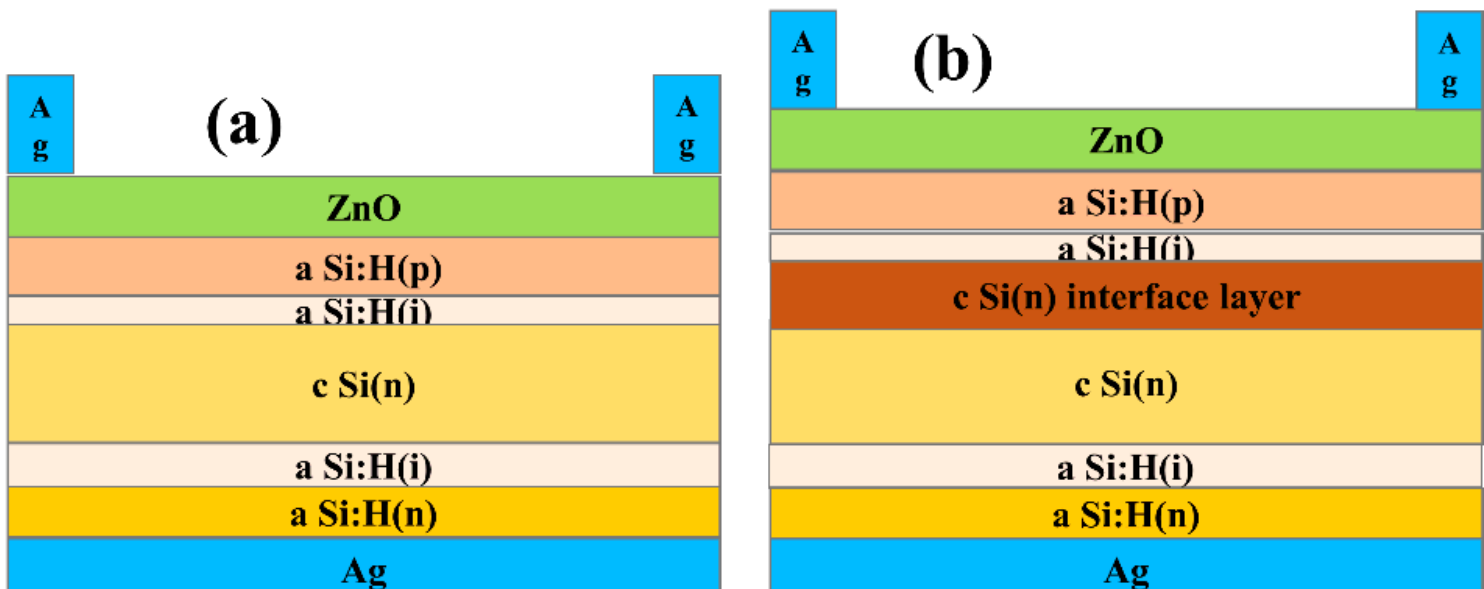


Figure 1

(a, b). Simulated c-Si/a-Si:H heterojunction solar cells structures.

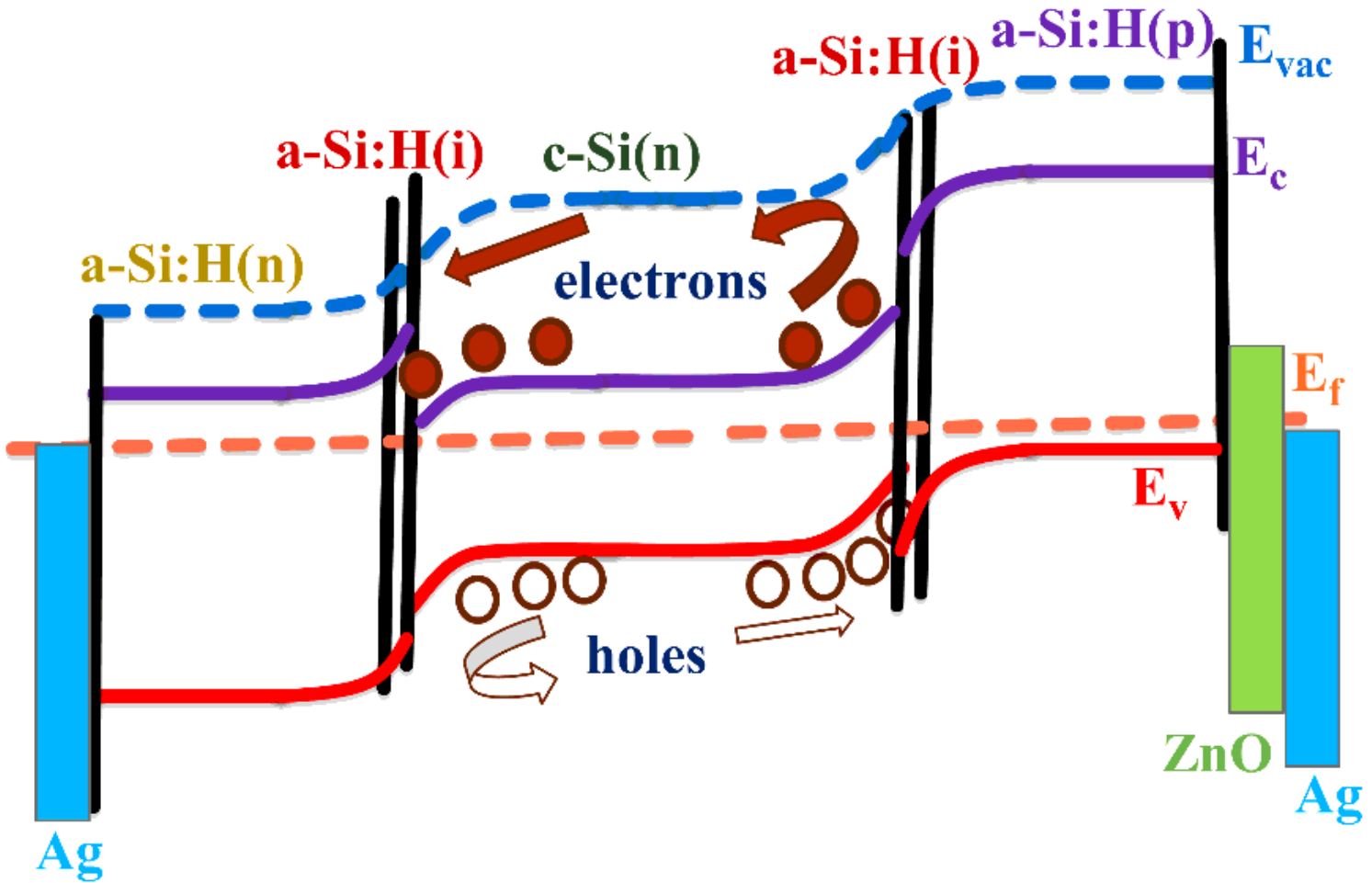


Figure 2

Band bending diagram of c-Si/a-Si:H heterojunction solar cells.

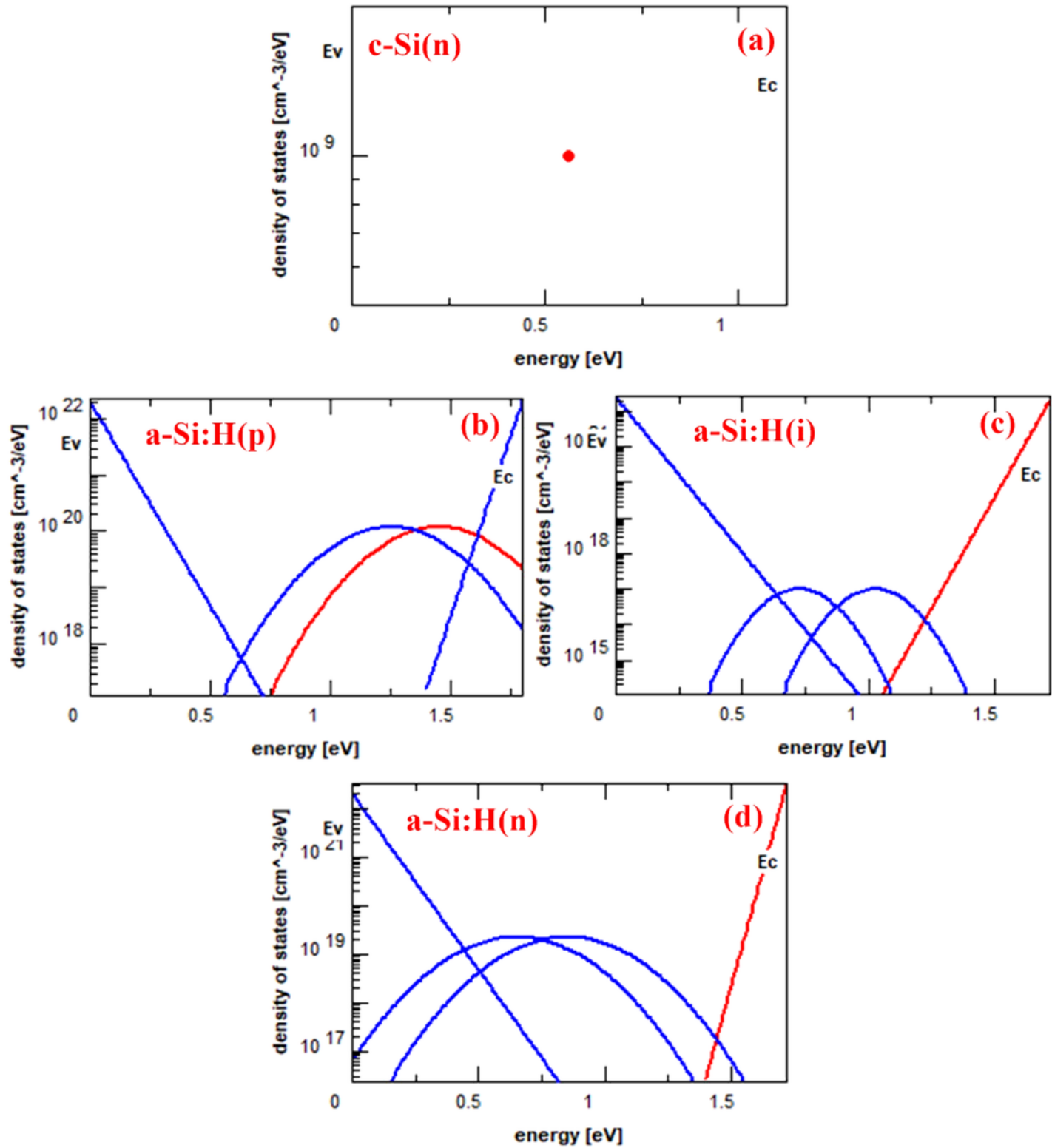


Figure 3

(a-d). Density of states as a function of energy of c-Si(n) wafer, a-Si:H(p), a-Si:H(i) and a-Si:H(n) layers.

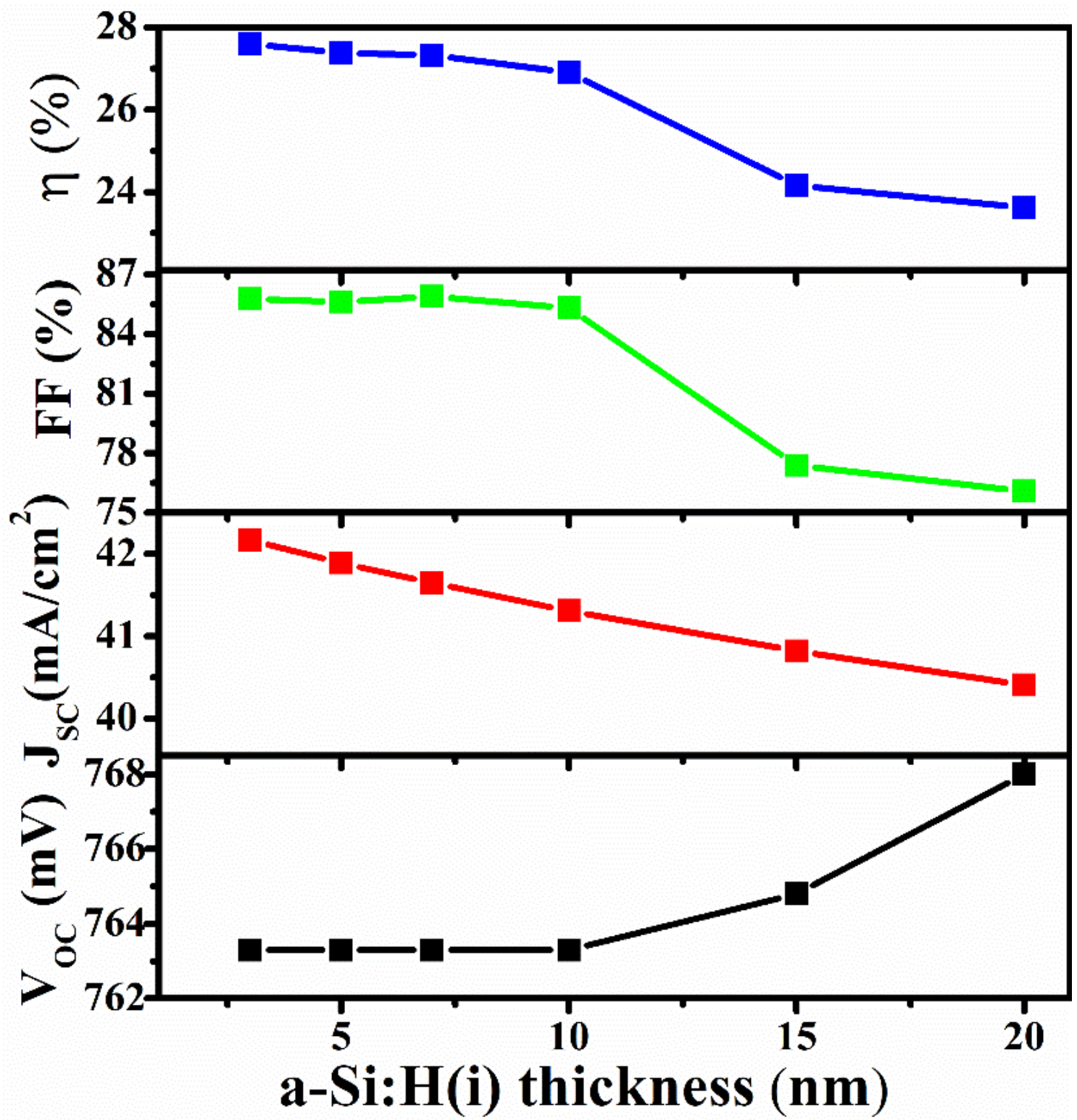


Figure 4

Solar cell parameters as function of a-Si:H(i) layer.

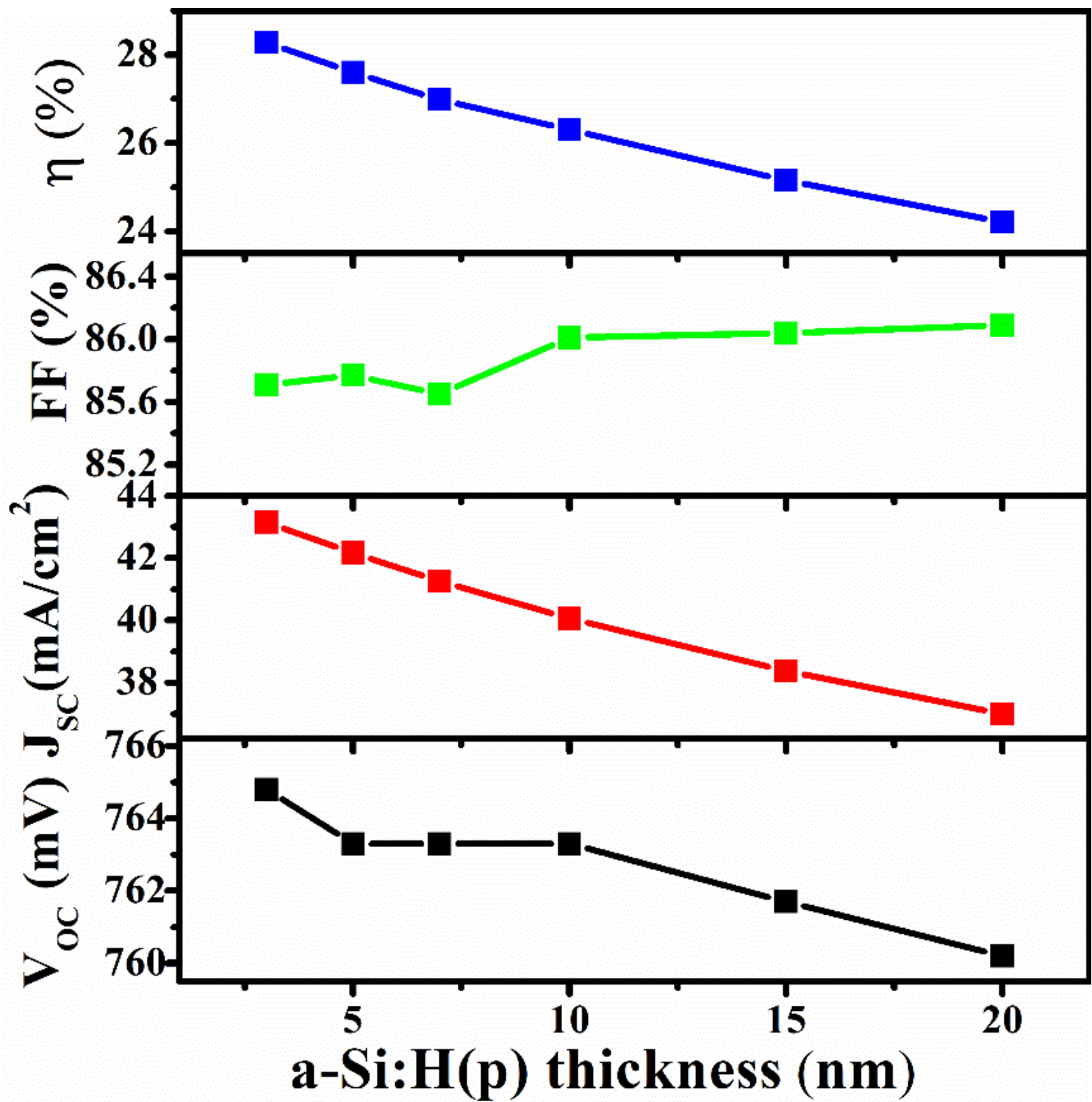


Figure 5

Solar cell parameters as function of a-Si:H(p) layer.

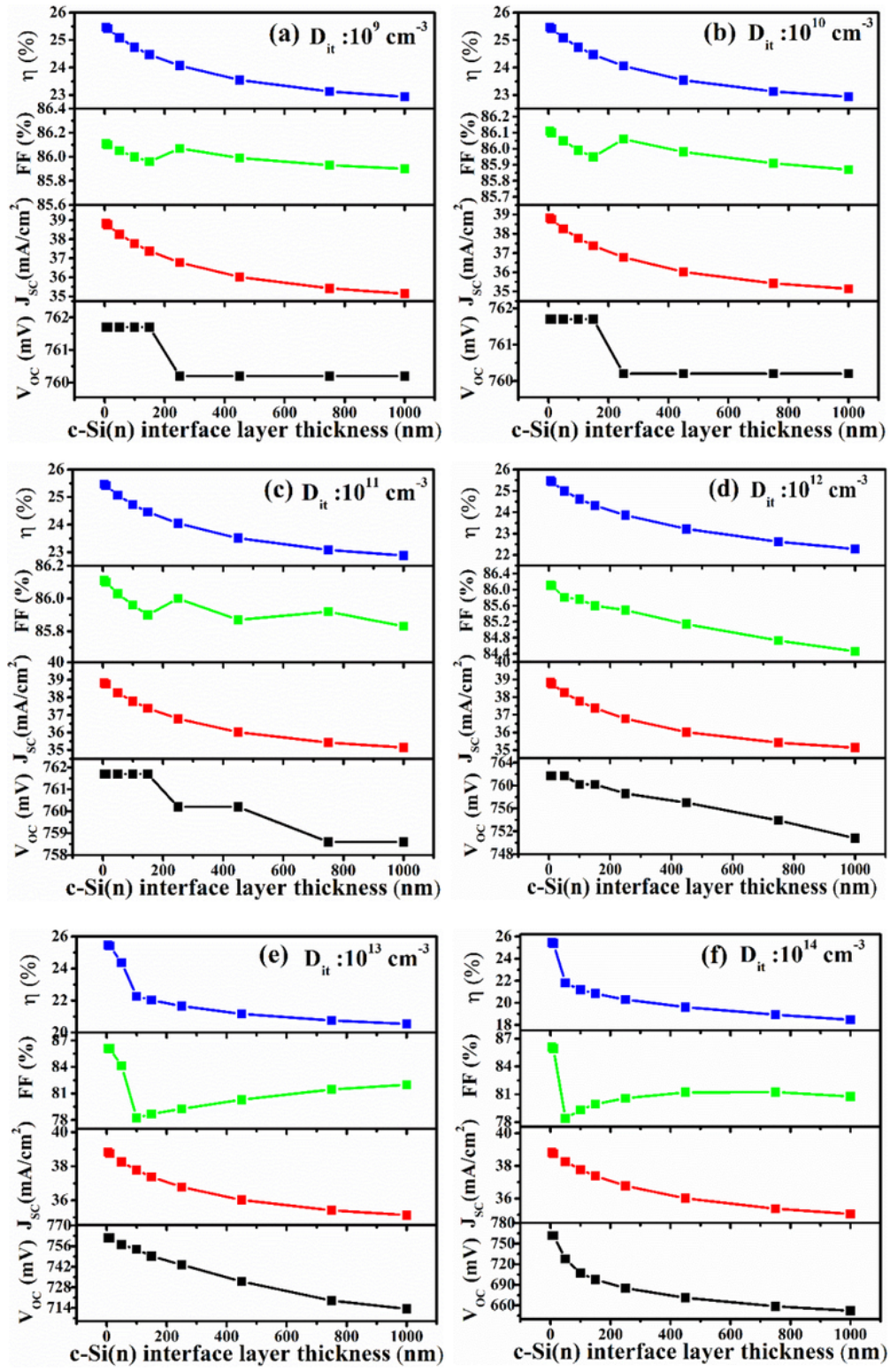


Figure 6

(a-f). Solar cell parameters as function of c-Si(n)interface layer thickness at defect density of 10⁹ to 10¹⁴ cm⁻³ respectively.

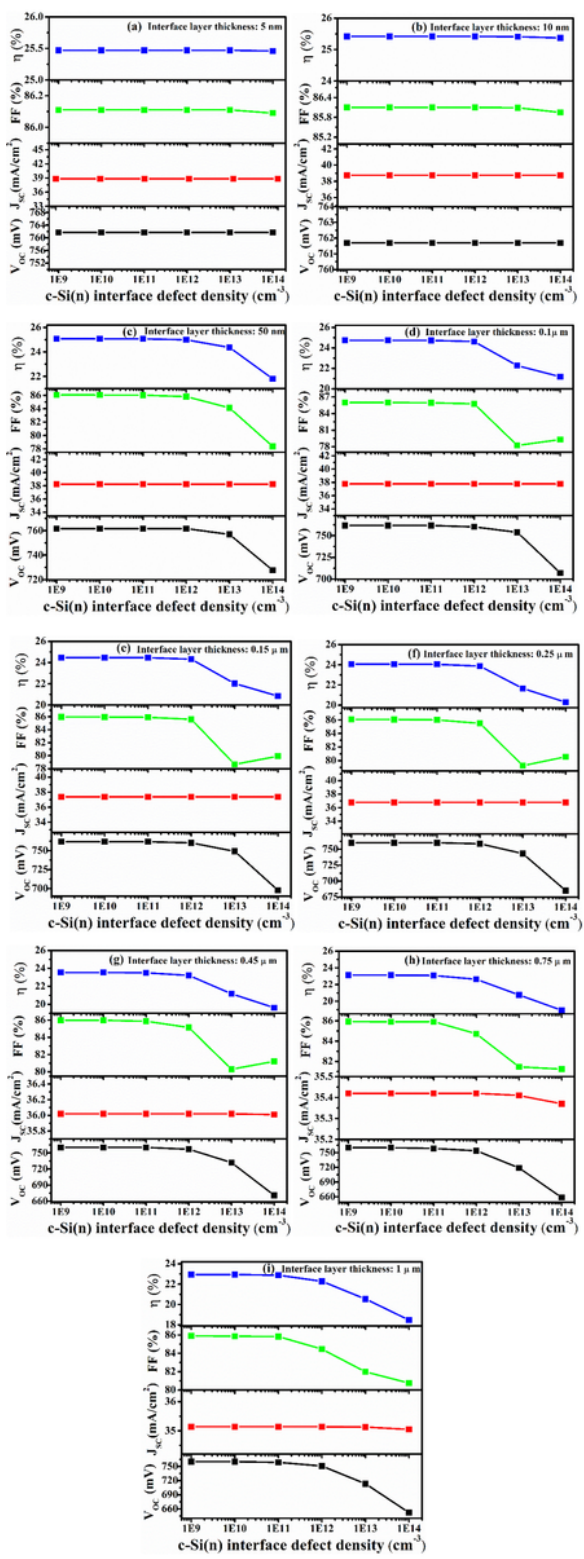


Figure 7

(a-i). Solar cell parameters as a function of c-Si(n)interface layer defect density at different thickness of interface layer respectively.